Electron-Dominated Spontaneous Bifurcation of Harris Equilibrium

Kuang-Wu Lee* and Jörg Büchner
Max-Planck-Institut für Sonnensystemforschung, 37191 Katlenburg-Lindau, Germany
(Dated: May 8, 2012)

In this letter the spontaneous bifurcation of Harris equilibrium current sheet is reported. The collisionless current bifurcation is simulated by a 2D particle-in-cell approach. Explicit particle advancing method is used to resolve the transient electron dynamics. Unlike previous implicit investigations no initial perturbations is applied to trigger current bifurcation. Instead, an electron-dominated spontaneously bifurcation is observed. Electromagnetic fluctuations grow from thermal noise initially. Soon the noise triggers the eigenmodes and eventually causes current sheet bifurcation. The relative entropy of the bifurcated state exceeds the value of initial Harris equilibrium. It is also found that the Helmholtz free energy decreases in the bifurcation process. Hence it is concluded that Harris equilibrium evolves toward a more stable (smaller free energy) bifurcated state.

PACS numbers: 05.70.-a, 05.70.Ce, 52.35.Ra:

Current sheet evolution plays a central role in astro- and laboratory- magnetic reconnection [1]. An analytical one-dimensional current sheet equilibrium was proposed by Harris [2] which has been since widely used as an initial configuration for space and laboratory current sheets.

Satellite observations of space current sheets, however, revealed in addition to single-peaked (Harris type) sheets, the existence of double- or multiple-peaked (bifurcated type) current sheet structures. The first in-situ evidence of magnetotail current sheet bifurcation was reported back in 1993 [3]. Statistical study of the spacecraft crossings in the terrestrial magnetotail pointed out that bifurcated current sheets are frequently observed [4][5]. Recently current sheet crossing data of other planets were revisited, e.g. the Jovian magnetotail crossing, back in the 1970's and 1990's by the Voyager-2 and Galileo spacecrafts. It was confirmed the existence of bifurcated current structures there [6]. These investigations indicate the multi-peak structures might be a rather typical current structures.

Assuming magnetic reconnection BCS has sometimes been interpreted as the indication of a pair of slow shocks in the outflow region [7][4][5] or as a tearing mode instability in elongated current sheets [8].

In addition to the interpretation of BCSs in magnetic reconnection, however, there is also observational evidence that BCS can exist at minimum plasma inflow condition. During a quiet solar wind condition magnetic reconnection is not expected to occur due to minimum inflow [9]. Up to now the detailed plasma transport in the original single-peaked current sheet is still an open question. Since BCSs might be due to different phenomena, there is no unified model for their formation.

Statistical magnetotail observation combined with MHD simulations interpreted BCS as an indication of magnetic reconnection [7]. The formation of BCS without plasma inflow, typical for reconnection, is however still under debate. In the current direction Daughton *et al.* [10] considered anomalous momentum transport due to the lower hybrid drift instability (LHDI), which is driven by pressure-gradient across current sheet [11]. In their work a semi-implicit numerical scheme was used and indeed, the LHDI eventually caused a bifurcation of the Harris current sheet. In the direction perpendicular to current direction a Harris equilibrium can evolve into BCS due to tearing mode instability [12]. In their 2D particle-in-cell (PIC) simulation an implicit numerical method is used for a faster particle advancing, and perturbations are imposed initially as seeds for the growth of tearing instability. The authors claimed that current sheet bifurcation took place after the tearing instability saturates. Assuming initial sheet boundary pressing, which is inspired by the satellite observations of BCS during strong solar wind condition, Schindler and Hesse [13] performed a one-dimensional particle-in-cell (1D PIC) simulation and concluded that current sheet bifurcation follows quasisteady boundary compression.

We conjecture that, despite of those simulations with the applied initial perturbation or boundary compression, spontaneous bifurcation can take place without disturbance on initial equilibrium. This is mainly due to the observational evidence that magnetotail current can bifurcate without obvious perturbations. Among the unsolved questions is the role of the electron in the bifurcation. An electromagnetic two dimensional particle-in-cell simulation (2D PIC) code is used to investigate the collisionless plasma dynamics in a single-peak Harris equilibrium. The numerical code implements an explicit scheme, i.e. it resolves the electron dynamics up to electron plasma/cyclotron frequency (ω_{pe} and Ω_{ce}).

The simulation background setup is a pure Harris sheet. The current sheet half-width λ is set to ion inertial length ($\lambda = d_i$) to cover the ion dissipation region of the current sheet. The equilibrium magnetic field is $B_y(x) = B_0 tanh(x/d_i) = \sqrt{4\mu k_B T N_0} tanh(x/d_i)$ where k_B, $T = T_i = T_e$, B_0 and N_0 are the Boltzmann constant, ion/electron temperatures, asymptotic magnetic field and number density at the center, respectively. By choosing T and N_0 the equilibrium magnetic field B_0 is determined. The ratio of electron plasma frequency to

* lee@mps.mpg.de

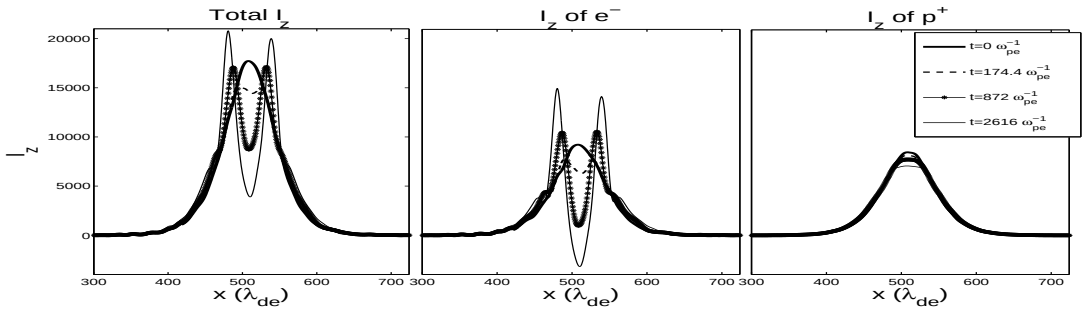

FIG. 1. The current profiles integrated in simulation y direction at different simulation times

electron cyclotron frequency is $\omega_{pe}/\Omega_{ce} = 2.87$. The ion to electron mass ratio used is $m_i/m_e = 180$, which is sufficient to separate the electron and ion dynamics. The grid should resolve the electron motion, therefore it size is set to Debye length $d_x = d_y = \lambda_{De} = (\varepsilon_0 T/Ne^2)^{1/2}$. The simulation domain across the inhomogeneity is $L_x = 23d_i$, while the length along the current sheet magnetic field $B_y(x) = B_{y,0}tanh(x/d_i)$ is $L_y = 46d_i$ direction. In order not to suppress the possible growth of tearing instability, the length L_y is chosen to allow the development of tearing instability with highest growth rate, which is predicted by the linear normal mode of Harris sheet (see Eq.(23) in [14]). The boundary conditions for the particles and fields are periodic in the y direction. Conducting wall with full particle reflection are imposed as the x boundary condition.

In order to consider the complete electron dynamics, an explicit numerical scheme is used for time advancing. For the time step used $dt = 0.0436\omega_{pe}^{-1}$ the Courant condition is fullfiled. This is much smaller than the time step used in the similar work with implicit numerical scheme [12] where $dt = 0.1\omega_{pi}^{-1} \approx 1.34\omega_{pe}^{-1}$ is used for a mass ratio $m_i/m_e = 180$. There is no initial perturbation imposed, which is different from the setup used e.g. in [12]. There reconnection was triggered by an initial perturbation of tearing mode scale. Also, our boundary condition prevents plasma compression imposed in the previous 1D PIC simulation of current bifurcation [13], where the initial boundary pressing (see Fig.1 therein) disturbs the initial Harris equilibrium and eventually causes bifurcation. The evolution of the Harris current density is shown in Fig.1. The current profiles are integrated along the y direction and they are shown as functions of x. The current profile exhibits a flattening of the density peak starting as early as at $t = 174\omega_{pe}^{-1}$. Split double-peaked current sheet is the next phase of flattening of current density. The gap between them also grows deeper at this phase. At the late stage $t = 2616\omega_{pe}^{-1}$ the two current peaks are completely separated. Interestingly, the fully developed current bifurcation observed here has developed fully at a relative early stage, which takes only a few ion cyclotron periods (ion cyclotron period is equivalent to Alfvén time, as used in [13]) $t = 872\omega_{pe}^{-1} \approx 1.6886\omega_{ci}^{-1}$. The bifurcation due to boundary pressing [13] appeared at $t \approx 400\omega_{ci}^{-1}$. The 2D PIC result shown here therefore proceeds faster. In [13] it was claimed that a current bifurcation must generally occur by quasisteady boundary compression if the initial current sheet is sufficiently wide. The question arises, what is the alternative driving force - if there in no boundary pressing - that disturbs the initial equilibrium?

To find out the alternative driving force for spontaneous bifurcation, it is appropriate to analyze the current distribution pattern in the simulation domain. As a result successively modulated current density was found, recognized as eigenmodes intrinsic of the Harris equilibrium. Due to the propagating eigenmodes in the Harris current sheet, where intrinsic waves can be triggered by thermal noises, the initial single-peaked current sheet splits and evolves into a more stable state. The characteristics of the linear eigenmodes are as follows.

First the evolution of current distribution in simulation is examined for which the current density in the out-of-plan direction (I_z) is plotted (see Fig.2). Both the total current (upper panels) and the electron contribution (lower panels) are shown at different simulation times. Initially the Harris current is concentrated near the center as it can be seen in the first column. At simulation time $t = 87.2\omega_{pe}^{-1}$ the wavs in the current distribution appear, shown as symmetric current patterns. At $t = 174.4\omega_{pe}^{-1}$ the amplitude of symmetric waves (about $y = 0$) becomes less pronounced. At the same time the current densities start to separate from each other distinctly. For the right column ($t = 1090\omega_{pe}^{-1}$) a clearly developed bifurcation can be seen. The wavy current sheet pattern has disappeared at this stage, indicating its role as an intermediate state for moving the system away from its original equilibrium. As already seen in integrated current profiles (Fig.1) the ions do not participate in the bifurcation process, therefore we do not show them here. This result confirms that even for an ion-to-electron mass ratio $m_i/m_e = 180$ the electron and ion dynamics are well separated. Note here that at later time ($t \approx 6000\omega_{pe}^{-1}$) the ion current contribution also bifurcates, similar to the simulation result obtained by using implicit numerical schemes or boundary compression/initial perturbations [12] [13]. In the following our simulation analysis will focus on the spontaneous bifur-

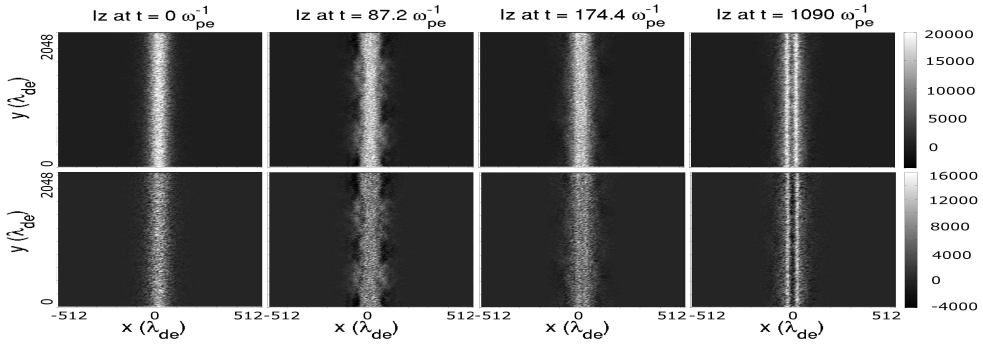

FIG. 2. The current distributions for different simulation times. The upper panels are the distributions for total current, and the lower panels are the electron contributions of the currents.

cation that is self-generated and dominated by the electron dynamics. The simulated current patterns should be compared with the eigenmodes of a Harris sheet. We use the linearized MHD dispersion relation for the eigenmode reconstruction. A generalized MHD dispersion relation for waves propating in non-uniform plasma was derived in [15]:

$$\frac{d}{dz}\left(f(z)\frac{d\xi_z}{dz}\right) = \varepsilon(z)\xi_z \tag{1}$$

where $f(z)$ and $\varepsilon(z)$ are defined in field-line coordinates

$$f(z) = -\rho(C_S^2 + C_A^2)\frac{(\omega^2 - k_{||}^2 C_A^2)(\omega^2 - k_{||}^2 C_{cp}^2)}{(\omega^2 - k_{||}^2 C_1^2)(\omega^2 - k_{||}^2 C_2^2)} \tag{2}$$

$$\varepsilon(z) = \rho(\omega^2 - k_{||}^2 C_A^2) \tag{3}$$

C_1, C_2 are $V_f/cos(\theta)$ and $V_s/cos(\theta)$. There V_f and V_s are phase velocities of fast- and slow- waves, and θ is the angle between $\vec{k}$ and $\vec{B}$. In the above equations $C_S^2 = \gamma P/\rho$, $C_A^2 = B^2/\mu_0\rho$ and $C_{cp}^2 = C_S^2 C_A^2/(C_S^2 + C_A^2)$ are the local sound speed, Alfvén speed and cusp speed of the current sheet, respectively. Eq.(1) is a 2nd order ordinary differential equation whose solution can be found for appropriate initial and boundary conditions. Finding the solution of Eq.(1) is equivalent to solving the eigenvalue problem. Symmetric eigenmodes can be found for the boundary conditions: 1) $\xi_z = a$ and $d\xi_z/dz = 0$ at current sheet center, for which it is a nonzero value, and 2) $\xi_z = 0$ at the current sheet edges. The first even eigenmodes are shown in Fig.3. The current density of the eigenmodes is distributed in a way as obtained by the simulation at its early stage (see column 2 of Fig.2). In both simulation and eigenmode calculation the perturbations propagate in the $\pm y$ direction, appearing as successively changing current intensity in Fig.2 and Fig.3. The wavelength of the modes is about $\lambda_y \approx 20 d_i$ and the current patterns agree well with each other. Note that the kinetic wave modes found in our PIC simulation do not directly correspond to the MHD eigenmodes of Harris sheet [15]. In fact, the charge separation and associated local electric fields are not described by MHD. Hence the

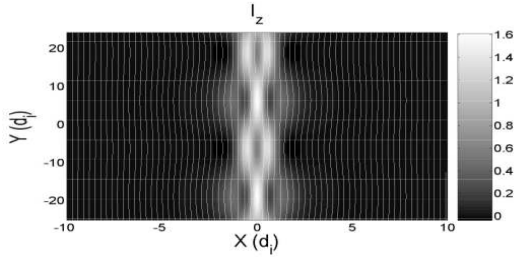

FIG. 3. Eigenmode of pure Harris sheet calculated according to [15]. The color indicates the current density of this mode, and the magnetic field is superposed.

Harris sheet eigenmodes should be described in a multi-fluid approach, which separately considers the ion and electron dynamics. To some extent the eigenmodes calculated from MHD dispersion relation, however, demonstrate the excited waves are intrinsic to the system with higher chances to survive.

Harris current sheet is a one-dimensional analytical equilibrium which assumed drift-Maxwellian distributions for electrons and ions with zero electric field [2]. Alternative, including non-analytical equilibria, have been long considered as more realistic for current sheets, if the restrictions of local drift-Maxwellian and zero electric field are removed [16]. A study of possible plasma distribution of current sheet equilibrium has been surveyed e.g. in [17]. The current density of proposed alternative equilibria has usually been solved numerically. Camporeale and Lapenta [12] have found numerous double- or multiple-peaked current sheet equilibria that are solutions of Vlasov-Maxwell equations.

Comparing the simulated current sheet bifurcation with numerically calculated equilibria, the bifurcated electron current sheet is similar to the one shown as case (b) in [12], with a single-peaked ion current and double-peaked electron current profile. Electron dominated current bifurcations are obtained also by magnetotail in-situ measurements. A statistical study of the current bifurcation using CLUSTER data has concluded that, the main carriers of bifurcated currents are electrons [18].

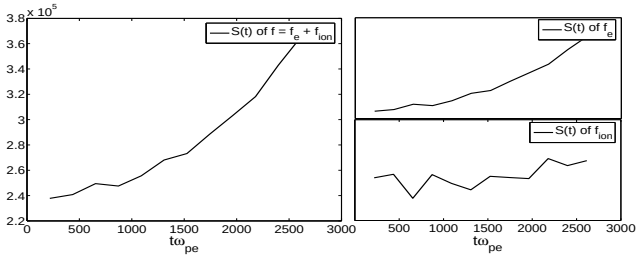

FIG. 4. Relative entropy of total distribution (left panel) and of individual electron (upper right panel) and ion (lower right panel).

Entropy is a quantity that measures the level of order in a system. For a plasma with continuous particle distribution, it is appropriate to consider a relative entropy which makes sure the entropy is always positive [19]. The relative entropy is defined as the Kullback-Leibler divergence $S_{KL}(t)$ with respect to a reference distribution $q(v)$ at $t = 0$.

$$S_{KL}(t) = \int_{-\infty}^{\infty} dv f(v,t) ln(\frac{f(v,t)}{q(v)|_{t=0}})$$

The entropy of a system in thermodynamical equilibrium has the highest entropy [20]. Indeed the relative entropy of the simulated 2D current sheet, the entropy of total distribution is increasing in the course of current sheet bifurcation (cf. Fig.4). The electron and ion entropies are plotted in the right columns. The entropy of electron is increasing while the ion/electron entropy oscillates. This is reasonable since the single species is not an isolated system. The total distribution is the sum of ions and electrons, and, therefore the total entropy of the current sheet increases in the course of bifurcation.

Equilibria are steady state solutions ($\partial/\partial t = 0$) of the Vlasov equation. Steady state solutions, however, might not correspond to a thermodynamical equilibrium but instead they are subject to various kinds of instabilities. A stability study of steady state equilibria can be done by calculating the Helmholtz free energy $F = U - TS$ of the system [21], in which the internal energy U is the sum of particle kinetic energy and the field energy, T is the temperature and S is the entropy. A more stable (or "less unstable") equilibrium corresponds to minimum free energy. In the bifurcation process, the internal energy U is conserved and T and S are increasing. Therefore, the bifurcated system has a lower free energy. This explains why the final bifurcated current sheet is a more favorable stable state than the single-peaked Harris equilibrium.

This 2D PIC simulation of an original Harris equilibrium has demonstrated that a spontaneous current bifurcation is a natural process which does not necessarily impose an initial perturbation to trigger tearing mode or another instability. Instead the electron causes a spontaneous bifurcation at an early stage of a Harris sheet evolution. This role of electron can be only found by using an explicit numerical scheme. This effect is even stronger if a real mass ratio is used. Intrinsic eigenmodes of the Harris sheet, self-consistently grown from thermal noise, act as perturbation and move the system away from its original equilibrium. This effect might explain the frequent observations of current sheet bifurcation even at locations, where the plasma inflow is small and magnetic reconnection is not expected.

The authors are grateful to the Max-Planck Society for funding this work under the Project No. MIF-IF-A-AERO 8047.

[1] J. Buechner, Plasma Phys. Control. Fusion **49**, B325 (2007).
[2] E. G. Harris, Nuovo Cimento **23**, 115 (1962).
[3] V. A. Sergeev, D. G. Mitchell, C. T. Russell, and D. J. Williams, J. Geophys. Res. **98**, 17,345 (1993).
[4] M. Hoshino, A. Nishida, T. Mukai, Y. Saito, T. Yamamoto, and S. Kokubun, J. Geophys. Res. **101**, 24,775 (1996).
[5] Y. Asano, R. Nakamura, W. Baumjohann, A. Runov, Z. Voros, M. Volwerk, T. L. Zhang, A. Balogh, B. Klecker, and H. Réme, Geophys. Res. Lett. **32**, L03108 (2005).
[6] P. L. Israelevich, A. I. Ershkovich, and R. Oran, Planet. Space Sci. **55**, 2261 (2007).
[7] S. M. Thompson, M. G. Kivelson, M. El-Alaoui, A. Balogh, H. Réme, and L. M. Kistler, J. Geophys. Res. **111**, A03212 (2006).
[8] W. Daughton, Phys. Plasmas **6**, 1329 (1999).
[9] C. L. Tang, L. Lu, Z. Y. Li, and Z. X. Liu, Chinese Phys. Lett. **23**, 1054 (2006).
[10] W. Daughton, G. Lapenta, and P. Ricci, Phys. Rev. Lett. **93**, 105004 (2004).
[11] J. Buechner and J. P. Kuska, Ann. Geophysicae **17**, 604 (1999).
[12] E. Camporeale and G. Lapenta, J. Geophys. Res. **110**, A07206 (2005).
[13] K. Schindler and M. Hesse, Phys. Plasmas **15**, 042902 (2008).
[14] M. Brittnacher, K. B. Quest, and H. Karimabadi, J. Geophys. Res. **100**, 3551 (1995).
[15] K. W. Lee and L. N. Hau, J. Geophys. Res. **113**, A12209 (2008).
[16] S. Cowley, Planet. Space Sci. **26**, 1037 (1978).
[17] K. Schindler and J. Birn, J. Geophys. Res. **107**, A8, 1193 (2002).
[18] P. L. Israelevich, A. I. Ershkovich, and R. Oran, J. Geophys. Res. **113**, A04215 (2007).
[19] S. Kullback and R. A. Leibler, Ann. Math. Statist. **22**, 79 (1951).
[20] E. T. Jaynes, Phys. Rev. **106**, 620 (1957).
[21] J. R. Kan, J. Plasma Phys. **7**, 445 (1954).